SCIENCE CHINA
Chemistry

• ARTICLES •
• SPECIAL TOPIC • Chemistry from Chinese Female Chemists

March 2015 Vol.58 No.3: 425–432
doi: 10.1007/s11426-015-5320-2

Ultrasensitive label-free electrochemiluminescence immunosensor based on *N*-(4-aminobutyl)-*N*-ethylisoluminol-functionalized graphene composite

Jiangnan Shu, Wen Shen & Hua Cui*

CAS Key Laboratory of Soft Matter Chemistry; Department of Chemistry, University of Science and Technology of China, Hefei 230026, China

Received September 22, 2014; accepted December 9, 2014; published online January 21, 2015

The electrochemiluminescence (ECL) behavior of *N*-(4-aminobutyl)-*N*-ethylisoluminol (ABEI)-functionalized graphene composite (ABEI-GC) modified on an indium tin oxide (ITO) electrode was studied. ABEI-GC exhibited excellent ECL activity. On this basis, a label-free ECL immunosensor was developed for the sensitive detection of human immunoglobulin G (hIgG) by using ABEI-GC as the ECL nano-interface via a layer-by-layer assembly technique. ABEI-GC was first assembled onto an ITO electrode. Positively charged chitosan was then electrostatically adsorbed to the modified electrode. Finally, negatively charged antibody-coated gold nanoparticles were attached to the surface to form the ECL immunosensor. In the presence of hIgG, hIgG was captured by its antibody. In addition, an ECL signal was detected in the presence of H_2O_2 when a double potential was applied. The ECL immunosensor for the determination of hIgG showed a linear range of 1.0×10^{-13}–1.0×10^{-8} g/mL with a detection limit of 5.0×10^{-14} g/mL. This immunosensor has high sensitivity, wide linearity and good reproducibility. The superior sensitivity of the proposed ECL immunoassay mainly derives from the incorporation of ABEI-GC, which not only improves the ECL intensity, response speed, and stability, but also provides a large specific surface for high levels of protein loading. This work reveals that ABEI-GC is good nano-interface for the construction of ECL biosensors. Our strategy is promising for protein detection and may open up a new avenue for ultrasensitive label-free immunoassays.

***N*-(aminobutyl)-*N*-(ethylisoluminol) (ABEI), graphene, electrochemiluminescence immunosensor**

1 Introduction

Immunosensors have attracted considerable attention so as to obtain quick and sensitive immunological responses for environmental monitoring, food safety, and clinical diagnoses [1,2]. However, conventional immunoassays based on labeling techniques are generally tedious, time-consuming, and costly, and may lead to the denaturizing of the modified biomolecules [3–5]. Therefore, there has been great interest in developing low-cost label-free biosensors. The main advantage of label-free strategies is that they do not require the labeling of the antibody or antigen with markers, which makes the experimental process simple, low cost, and time-saving. Label-free immunoassays combined with various detection techniques such as piezoelectricity [6], surface plasmon resonance [7], electrochemistry [8], chemiluminescence (CL) [9], and ECL [10,11] have been developed.

As a valuable detection method, ECL has been widely applied to clinical diagnosis, environment monitoring, food safety, and pharmaceutical analysis due to acknowledged advantages such as versatility, simplified optical setup, very low background signal, and good temporal and spatial control [12–16]. Recently, label-free ECL immunoassays have also been reported for the determination of small molecules and biomacromolecules and have shown high sensitivity,

*Corresponding author (email: hcui@ustc.edu.cn)

specificity, rapidity, simplicity, and low cost [11,17].

Recently, graphene has attracted considerable attention due to its high electrical conductivity, high surface-to-volume ratio, high electron-transfer rate, and exceptional thermal stability [18,19]. To expand the use of graphene in various applications, much effort has been made in terms of its functionalization so as to obtain advanced functional composites with superior characteristics [20–22]. In our previous work, graphene was successfully functionalized with ABEI via π-π interactions that exhibited good CL activity [23]. In view of the high electrical conductivity and electrocatalytic activity of graphene and the good ECL activity of ABEI, such composites might also possess good ECL characteristics. In addition, graphene has the advantages of high surface-to-volume ratio and good biocompatibility, which are beneficial to the construction of biosensing platforms. Accordingly, it provides a strong possibility for developing an ultrasensitive label-free ECL immunosensor based on ABEI-GC as the nano-interface.

We studied the ECL behavior of an ABEI-GC-modified ITO electrode. The ABEI-GC-modified ITO electrode in alkaline solution exhibited good ECL activity in the presence of H_2O_2. On this basis, we proposed a label-free ECL immunosensor by using ABEI-GC as the nano-interface via a layer-by-layer assembly method that takes hIgG as a model target. The fabrication of the immunosensor was studied by electrochemical impedance spectroscopy (EIS). The conditions for ECL detection were optimized. The analytical performance and the specificity of the immunosensor were examined. The applicability of the proposed immunosensor in real human-serum samples was investigated.

2 Experimental

2.1 Materials and chemicals

ABEI was purchased from Sigma-Aldrich (USA). Graphene oxide (GO) was purchased from XFNANO Materials Tech Co. Ltd. (Nanjing, China). Bovine serum albumins (BSA), hIgG, and goat-antihuman IgG were obtained from Solarbio (Beijing, China). Chloroauric acid ($HAuCl_4{\cdot}4H_2O$) was obtained from Shanghai Reagent Company (Shanghai, China). A $HAuCl_4$ stock solution (2% $HAuCl_4$, *w*/*w*) was prepared by dissolving 1.0 g of $HAuCl_4{\cdot}4H_2O$ in 412 mL of purified water and storing the mixture at 4 °C. Chitosan (95% deacetylation) was prepared by dissolving chitosan in 0.1 mol/L acetic acid solution, filtering the insoluble substance, and adjusting the pH to 5.0 with 0.1 mol/L sodium hydroxide solution. The buffer solutions used in the experiment included carbonate buffer (CBS, $NaHCO_3$-Na_2CO_3) and phosphate saline buffer (PBS). All of the other reagents were of analytical grade. Ultrapure water was prepared by a Milli-Q system (Milli-pore, France) and used throughout.

2.2 Apparatus

Electrochemical and ECL measurements were performed with a homemade ECL/Electrochemical cell system, including a model CHI 760B electrochemistry work-station (Chenhua, China), an H-type electrochemical cell (homemade) [24], a model CR-105 photomultiplier tube (PMT) (Bingsong, China) and a model RFL-1 luminometer (Ruimai, China). The EIS experiment was performed with a CHI 760B electrochemistry workstation (Chenhua, China). A PST-60 HL plus Thermo Shaker (Biosan, Latvia) was used to control the temperature of the reactions.

2.3 Preparation of ABEI-GC

The ABEI-GC was synthesized as described previously [23]. First, 5 mL (2 mg/mL) of aqueous ABEI alkaline solution was added to 5 mL (0.2 mg/mL) of exfoliated GO suspension. After ultrasonication for 30 min, the mixture was vigorously stirred at 80 °C for 24 h. Next, the dialysis procedure was used to remove the free ABEI and the coexisting free molecules from the ABEI-GC dispersion.

2.4 Preparation of goat-anti-human IgG-AuNPs

Gold nanoparticles (AuNPs) were prepared by the trisodium citrate reduction method according to a previous study, with modification [25]. Briefly, 5.0 mL of 1% trisodium citrate solution was rapidly added to 100 mL 0.3 mmol/L boiling $HAuCl_4$ solution with fierce stirring. The mixture was refluxed for 30 min and then naturally cooled to room temperature. After being filtered through a 0.22 μm cellulose membrane, the AuNPs solution was adjusted to pH 8.0 with diluted NaOH solution. The goat-antihuman IgG functionalized AuNPs (Ab-AuNPs) were prepared according to previously reported studies, with modification via electrostatic interaction as well as hydrophobic interaction and weak covalent interactions [5,26]. Next, 25 μL of 1.0 mg/mL goat-antihuman IgG antibody was added to 1.0 mL of the pH 8.0 AuNPs solution, followed by incubation at room temperature for 30 min. The solution was added, with 5% BSA solution, to the final concentration of 1% BSA and then stirred for 5 min. The conjugate was centrifuged at 17120 r/min for 40 min (Universal 320, Hettich, Germany) to remove the excess reagent, and the soft sediment was dissolved in PBS buffer (0.1 mol/L, pH 7.4) containing 1% (*w*/*w*) BSA to obtain the Ab-AuNPs. A CD experiment demonstrated that the Ab was successfully conjugated to the AuNPs.

2.5 Fabrication of label-free ECL immunosensor

ITO-coated glass slides were used as assembly electrodes owing to their stability, easy miniaturization, and compatibility with microfabrication [27]. ITO-coated glass slides

with dimensions of 6.0 cm×1.5 cm were cleaned by sequential sonication in neat acetone, ethanol, and ultrapure water (15 min each). The ITO substrate was reversibly bound to a punched poly(dimethylsiloxane) (PDMS) layer that was prepared by curing the mixture of PDMS monomer and the curing agent (10:1) in an oven at 75 °C for 1.5 h. The effective electrode area was confined by a punched round hole of 5 mm in diamter, which was used as a reservoir for subsequent assembly.

The ECL immunosensor was assembled via the layer-by-layer method (Figure 1). First, 50 μL ABEI-GC solution was dropped into the reservoir and dried naturally in air. Then, 10 μL 5% chitosan solution was dropped onto the ABEI-GC modified electrode and dried in air. Later, the modified electrode was rinsed with ultrapure water to remove the physically adsorbed chitosan. Subsequently, 50 μL Ab-AuNPs solution was added to the reservoir and incubated at 4 °C for 8 h and rinsed again with ultrapure water. Next, 50 μL 1% (*w*/*w*) BSA in 0.01 mol/L PBS (pH 7.4) was used for blocking non-specific binding sites for 30 min at 37 °C, followed by a thorough washing with 0.02 mol/L PBS. Finally, 50 μL of different concentrations of hIgG were dropped on the modified electrode at 37 °C for 40 min, followed by a thorough washing with 0.02 mol/L PBS. In this way, the hIgG/BSA/Ab-AuNPs/CS/ABEI-GC/ITO-modified ITO substrate (i.e., the immunosensor) was successfully constructed.

2.6 ECL measurement

ECL measurements were carried out on a three-electrode homemade ECL system. The modified ITO electrode described above served as the working electrode; a platinum wire served as the counter-electrode; and a silver wire served as the quasireference electrode (AgQRE). We chose to use an AgQRE due to the simplicity of its cell construction and quick potential response. Although the potential of the AgQRE was found to be essentially stable during an experiment, measurements of $\Delta E=E_{Ag/Ag+}-E_{SCE}$ in different solutions were taken for potential calibrations. During the ECL measurements, a portion of the CBS buffer (0.02 mol/L, pH 9.95) containing 1 mmol/L H_2O_2 was transferred into the working compartment and the auxiliary compartment of the ECL cell. When a double-step potential (30 s pulse period, 0.1 s pulse time, 0.6 V pulse potential, and 0 V initial potential) was applied to the working electrode, the ECL signal was generated and recorded.

3 Results and discussion

3.1 ECL behaviors of the ABEI-GC nano-interface

The electrochemical and ECL behaviors of ABEI-GC-modified ITO electrode were studied. Cyclic voltammograms (CVs) were taken from 0 to 1.0 V in 0.02 mol/L CBS (pH 9.95) containing 1 mmol/L H_2O_2. In Figure 2, Curves a and b respectively depict the curves of ECL intensity versus the potential and CV of the ABEI-GC-modified ITO electrode. The ABEI-GC modified ITO electrode exhibited good ECL activity. The ECL emission started at 0.25 V and the ECL peak value was achieved at around 0.7 V; the latter was related to electro-oxidation of ABEI on the ITO electrode according to the CV of pure ABEI (Figure 2, Curve c). These results indicated that the ECL emission was from ABEI molecules attached on the surface of graphene. Therefore, it is feasible to fabricate a label-free ECL immunosensor based on such an ECL functionalized nano-interface.

We also studied the ECL behavior of ABEI-GC under a double-step potential on the ABEI-GC-modified ITO electrode in 0.02 mol/L CBS (pH 9.95) containing 1 mmol/L H_2O_2 (Figure 3). When the double-step potential was applied to the electrode, a pulse ECL signal was obtained. Figure 3 displays the ECL signals for 10 periods, which were much better than those obtained by CV in both signal

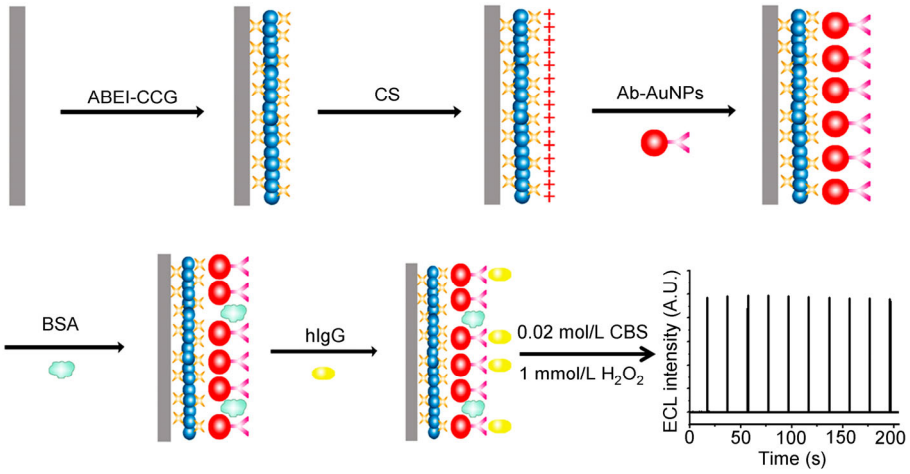

Figure 1 Schematic illustration of the fabrication process and detection of a label-free ECL immunosensor for hIgG detection.

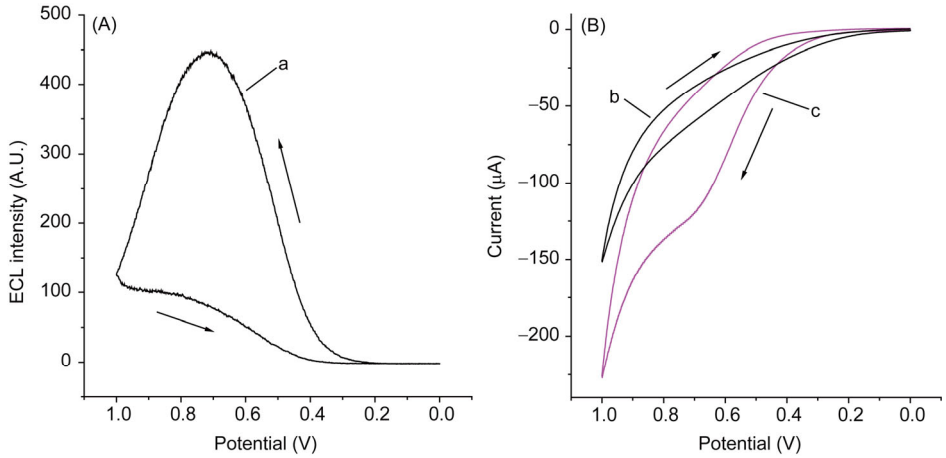

Figure 2 (A) Curve of ECL intensity versus potential of ABEI-GC-modified ITO electrode (Curve a); (B) CV profiles of ABEI-GC modified ITO electrode (Curve b) and pure ABEI (Curve c). The potential was scanned from 0 to 1.0 V in 0.02 mol/L CBS (pH 9.95) containing 1 mmol/L H_2O_2.

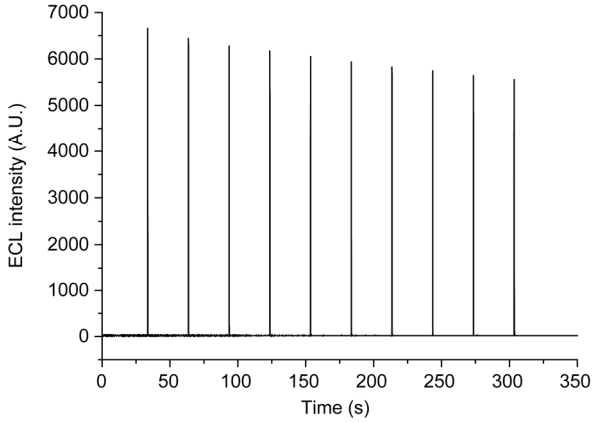

Figure 3 ECL signals of ABEI-GC-modified ITO electrode under a double-step potential in 10 pulse periods. Experimental parameters: initial potential, 0 V; pulse potential, 0.6 V; pulse time, 0.1 s; pulse period, 30 s; H_2O_2 concentration, 1.0 mmol/L; CBS, 0.02 mol/L (pH 9.95).

intensity and stability. Therefore, double-step potential was chosen for the immunosensor in the following experiments.

3.2 Construction and characteristics of the label-free ECL immunosensor

Figure 1 displays the procedure and the working prinicple for fabricating a label-free ECL immunosensor for human immunoglobulin detection. First, ABEI-GC was self-assembled on the surface of the ITO substance through physical absorption, to provide ECL-functionalized nano-interface. Next, positively charged chitosan was adsorbed to the nano-interface of the ABEI-GC through electrostatic interaction. After that, negatively charged Ab-AuNPs were further assembled on the ABEI-GC-modified electrode via electrostatic interaction. Next, BSA was used for blocking the non-specific binding sites. Finally, hIgG was attached on the modified electrode via specific binding between goat-antihuman IgG and hIgG.

EIS was used to monitor the process of electrode modification (Figure 4). The results were consistent with the fact that the electrode was modified as expected. The impedance spectra consisted of a semicircle at high ac modulation frequency and a line at low ac modulation frequency, which demonstrated that the electrode process was controlled by electron transfer at high frequency and by diffusion at low frequency. The electron transfer resistance decreased with the decrease of the diameter of the semicircle. Our stepwise EIS measurements of the modified ITO electrode at different modification steps were carried out at the PDMS reservoir because this placement ensured the same electrode area. It can be seen that when ABEI-GC was assembled on the ITO electrode, the electron transfer resistance increased remarkably (Curve b) compared with the bare ITO electrode (Curve a). After further modification with chitosan, an insulating layer was created on the surface of as-prepared electrode, resulting in an increased electron transfer resistance (Curve c). Once the Ab-AuNPs were further assembled on the electrode (Curve d), the electron transfer resistance decreased significantly due to the superior conductivity of AuNPs, which facilitated the electron transfer between the protein active center and the electrode surface and led to a net decrease in electron transfer resistance. After further incorporation of BSA, the electron-transfer resistance elevated largely as expected (Curve e), because the proteins blocked the electron transfer. Therefore, we increased the electron transfer resistance after more hIgG was attached to the surface of the modified electrode (Curve f). The entire EIS dataset indicated that the electrode was modified as expected.

The process of electrode modification was also investigated by the ECL behavior of each step. The ECL responses of the modified electrodes at different stages were examined as shown in Figure 5. Strong ECL signals were observed after the ABEI-GC was assembled on the ITO electrode (Curve a), because of the good ECL property of ABEI-GC.

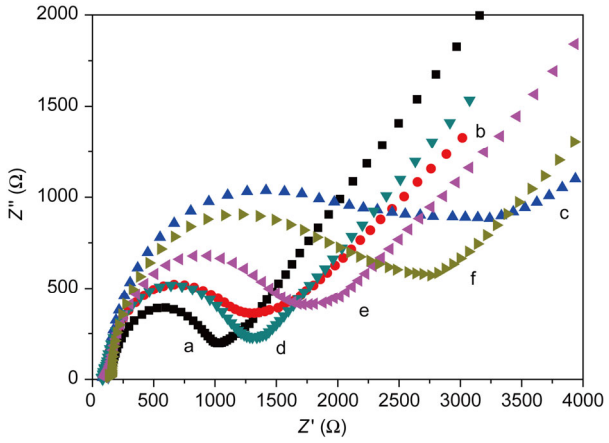

Figure 4 Nyquist plot for the Faradaic impedance measurements of the modified ITO electrode by layer-by-layer self-assembly in PBS (0.1 mol/L, pH 7.0) containing $[Fe(CN)_6]^{3-}$+$[Fe(CN)_6]^{4-}$ (both 1×10^{-3} mol/L). (a) Bare ITO surface; (b) ABEI-GC/ITO; (c) CS/ABEI-GC/ITO; (d) Ab-AuNPs/CS/ABEI-GC/ITO; (e) BSA/Ab-AuNPs/CS/ABEI-GC/ITO; (f) hIgG/BSA/Ab-AuNPs/CS/ABEI-GC/ITO.

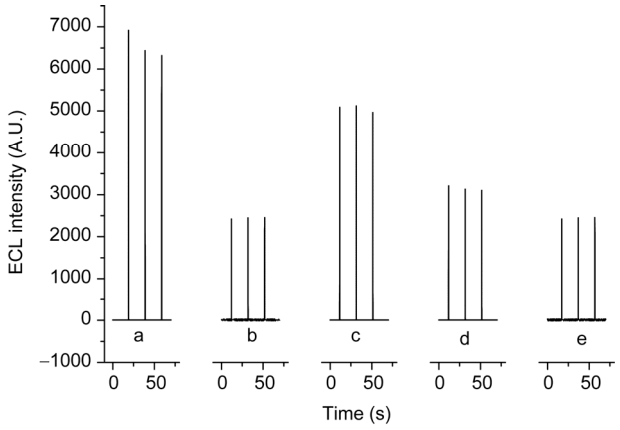

Figure 5 ECL signals under pulse potential obtained with (a) ABEI-GC/ITO, (b) CS/ABEI-GC/ITO, (c) Ab-AuNPs/CS/ABEI-GC/ITO, (d) BSA/Ab-AuNPs/CS/ABEI-GC/ITO, (e) hIgG/BSA/Ab-AuNPs/CS/ABEI-GC/ITO. Initial potential, 0 V; pulse period, 30 s; pulse time, 0.1 s; pulse potential, 0.6 V; H_2O_2, 1.0 mmol/L; CBS, 0.02 mol/L (pH 9.95).

When assembled with chitosan, the ECL intensity decreased dramatically, owing to the insulating property of chitosan (Curve b). The ECL intensity increased significantly after Ab-AuNPs were assembled on the electrode (Curve c), which contributed to the superior conductivity and the catalytic characteristics of AuNPs. After bounding with BSA, the ECL intensity was much reduced because the proteins blocked the electron transfer (Curve d). Similarly, the ECL intensity decreased after further incorporation of hIgG (Curve e). Accordingly, we might quantitatively evaluate the concentration of hIgG according to ECL response.

3.3 Optimization of experimental conditions

A double-step potential was applied to the electrode to initiate the ECL signal of the immunosensor in the presence of H_2O_2 (Figure 1). To obtain optimal ECL signaling, the effects of pH value, pulse period, pulse time, pulse potential, initial potential, and concentration of H_2O_2 on the ECL intensity should be investigated. The effect of pH on the ECL intensity was examined in the range of 8.95–11.37 in 0.02 mol/L CBS. Figure 6(a) shows the pH dependence of the ECL intensity; maximal ECL intensity was obtained at pH 9.95. The effect of the initial pulse potential in the range of –0.3–0.3 V was also investigated (Figure 6(b)). When the initial pulse potential was 0 V, maximal ECL intensity was achieved; probably because the initial pulse potential of 0 V had a better diffusion controlled reaction on the surface of the modified electrode. Therefore, an initial pulse potential of 0 V was used in the following experiments. The effect of the pulse potential in the range of 0.4–0.8 V was studied as well (Figure 6(c)). The ECL intensity increased with the increase of the pulse potential because the electro-oxidation was much faster at higher electrode potential. A pulse potential of 0.6 V was adopted because the stability and reproducibility of the modified electrode declined if a high potential (above 0.6 V) was used. The effect of pulse time on the ECL intensity was examined in the range of 0.025–0.125 s (Figure 6(d)). The ECL intensity increased with the pulse time. However, when the pulse time was longer than 0.1 s, the ECL intensity decreased rapidly at the second period and could not reach a stable ECL signal in the following period. This result occurred because the diffusion layer on the surface of electrode became thicker in a relatively long pulse time and could not recover in the next pulse. Therefore, a pulse time of 0.1 s was selected. The effect of the pulse period on the ECL intensity was investigated in the range of 10–50 s (Figure 6(e)). The ECL intensity increased with the pulse period, which might have been due to more-effective diffusion of H_2O_2 in a longer pulse period. To obtain a shorter analytical time and higher ECL intensity, a pulse period of 30 s was adopted in the following experiments. The ECL intensity increased with the increase of the concentration of H_2O_2 and reached maximum at 1.0 mmol/L (Figure 6(f)). Therefore, 1.0 mmol/L H_2O_2 was used in the following experiments.

3.4 Analytical performance of the label-free ECL immunosensor

Under the optimized conditions, label-free ECL immunosensor was employed for the detection of hIgG. The ECL signal increased with the increment of hIgG concentration (Figure 7), which exhibited a wide linear dynamic range of 1.0×10^{-13}–1.0×10^{-8} g/mL. The regression equation was I=–3417.1–529.3log$C$ and the correlation coefficient was 0.996, where I was the ECL intensity and C was the concentration of hIgG (g/mL). The limit of detection for hIgG at a signal-to-noise ratio of 3 (S/N=3) was 5.0×10^{-14} g/mL. The precision of the ECL immunosensor was also investi-

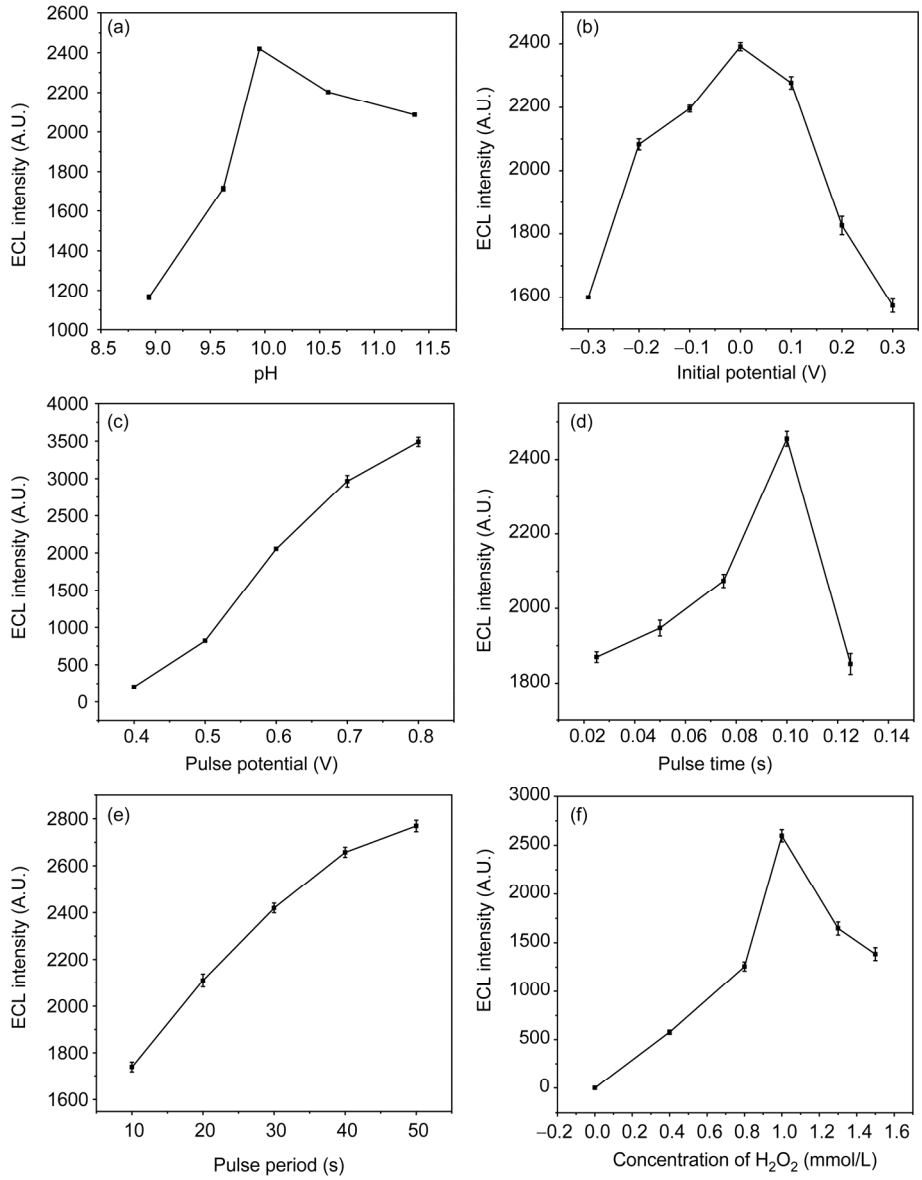

Figure 6 Effect of (a) pH, (b) initial pulse potential, (c) pulse potential, (d) pulse time, (e) pulse period, (f) H_2O_2 concentration on ECL intensity of immunosensor. Initial potential, 0 V; pulse potential, 0.6 V; pulse time, 0.1 s; pulse period, 30 s; H_2O_2 concentration, 1.0 mmol/L; CBS, 0.02 mol/L (pH 9.95).

gated. The relative standard deviations (RSD) of five replicate determinations of hIgG within a day (intra-day precision, n=5) was 3.27%; the RSD in 7 days (inter-day precision, n=7) was 8.03%. These results indicated acceptable reproducibility.

To affirm the specificity of the label-free ECL immunosensor, BSA, lysozyme, hemoglobin (HGB), and human serum albumin (HSA) with 1.0×10^{-9} g/mL concentration were chosen as interferents. They were used for immunoassays instead of hIgG. As can be seen in Figure 8, the ECL response from BSA, lysozyme, HGB, and HSA with concentrations of 10× over hIgG were comparable with the blank. A much weaker ECL response was observed when 1.0×10^{-10} g/mL hIgG was used for the ECL immunoassay. These results demonstrate that the developed label-free ECL immunosensor is selective for the detection of hIgG.

A comparison of the proposed method with other label-free immunoassays for the determination of hIgG was made (Table 1) [1, 28–33]. The results show that the limit of detection of the present method is superior to most previously reported methods for the determination of hIgG. Although the present label-free ECL immunosensor exhibited a higher detection limit than the assays based on graphene-quantum dots composites amplification via the conjugation of PDDA and GNPs, it avoided complicated experimental procedures. This avoidance made the method low cost, easy to operate, and time-saving. Moreover, the present method showed good precision as well as acceptable stability and reproducibility. Therefore, the proposed method is promising for practical applications in fields such as clinical diagnosis,

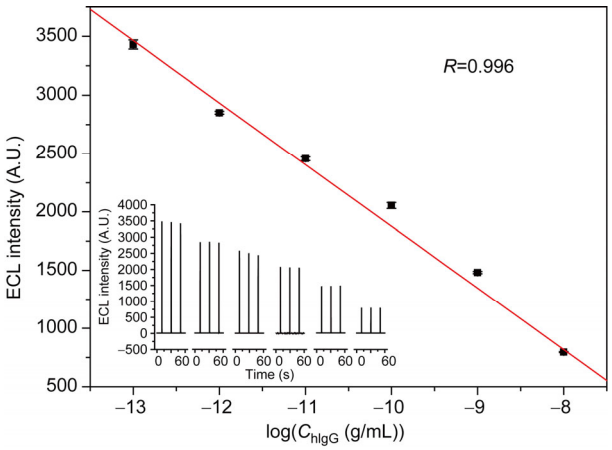

Figure 7 Calibration curve for hIgG. Initial potential, 0 V; pulse period, 30 s; pulse time, 0.1 s; pulse potential, 0.6 V; H_2O_2, 1.0 mmol/L; CBS, 0.02 mol/L (pH 9.95). Inset: ECL signals of label-free immunosensor at different hIgG concentrations.

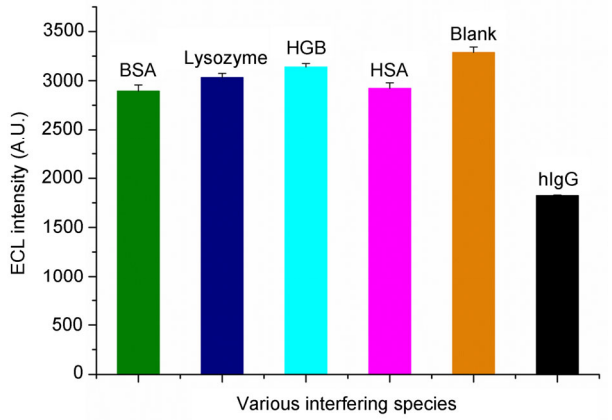

Figure 8 A comparison of ECL responses of hIgG with those of different interfering species. 1.0×10^{-9} g/mL BSA; 1.0×10^{-9} g/mL lysozyme; 1.0×10^{-9} g/mL HGB; 1.0×10^{-9} g/mL HSA; blank. Initial potential, 0 V; pulse period, 30 s; pulse time, 0.1 s; pulse potential, 0.6 V; H_2O_2, 1.0 mmol/L; CBS, 0.02 mol/L (pH 9.95).

Table 1 A comparison of proposed label-free ECL immunoassay protocol with other label-free immunoassays for the determination of hIgG

Type	Amplification	Detection method	LOD (pg/mL)	Reference
$[Fe(CN)_6]^{3-}$		electrochemical	3000	[28]
PoPD		EIS	50	[29]
ABEI-GC	AuNPs	ECL	0.05	this work
CdS QDs	PDDA	photoelectro-chemical	8	[1]
protein A		EIS	5000	[30]
AgTNPs		LSPR	2000	[31]
nano-Au-ERGO	AuNPs	ECL	1.3	[32]
P-GR-CdSe	PDDA/AuNPs	ECL	0.005	[33]

environment monitoring, food safety, pharmaceutical analysis, etc.

Table 2 hIgG content in human serum samples measured by the proposed method and recovery of hIgG in human-serum samples

Sample	hIgG found (10^{-10} g/mL)	hIgG added (10^{-10} g/mL)	Total hIgG detected (10^{-10} g/mL)	Recovery (%)
1	9.4	10	19.1	97
2	10.3	10	20.5	102
3	12.0	10	22.4	104

3.5 Application of label-free ECL immunosensor in human serum samples

The clinical applicability of the proposed method was investigated by analyzing several real samples of human serum. Before the test, the samples were appropriately diluted step by step to be in the linear range of the proposed method. As shown in Table 2, the recoveries were in the range of 97%–104%, which indicated that the developed label-free ECL immunoassay could be applied for the determination of hIgG in clinical diagnosis.

4 Conclusions

An advanced label-free ECL immunosensor is proposed for the sensitive detection of hIgG by using ABEI-GC to build a CL-sensing platform. Due to the high conductivity and the electrocatalytic activity of the graphene-based immunosensor as well as the superior ECL property of ABEI-GC, trace amounts of hIgG were successfully determined by the as-prepared immunosensor with good ECL response. Furthermore, the large specific surface area of graphene afforded high protein loading and the gold nanoparticles could further enhance the ECL intensity. As a result, the sensor showed an extremely sensitive response to hIgG in a linear range of 1.0×10^{-13}–1.0×10^{-8} g/mL with a detection limit of 5.0×10^{-14} g/mL. Moreover, the label-free ECL immunosensor showed good precision as well as acceptable stability and reproducibility, which indicate great potential in clinical applications. This research provides a promising technique for protein detection, which may open up a new avenue for ultrasensitive label-free immunoassays.

This work was supported by the National Natural Science Foundation of China (20625517, 21075115, 21173201), the Merieux Research Grants, the Fundamental Research Funds for the Central Universities (WK2060190007) and the Opening Fund of the State Key Laboratory of Electroanalytical Chemistry, Changchun Institute of Applied Chemistry, Chinese Academy of Sciences (SKLEAC201408).

1 Wang GL, Yu PP, Xu JJ, Chen HY. A label-free photoelectrochemical immunosensor based on water-soluble Cds quantum dots. *J Phys Chem C*, 2009, 113: 11142–11148

2 Tsagkogeorgas F, Ochsenkuhn-Petropoulou M, Niessner R, Knopp D. Encapsulation of biomolecules for bioanalytical purposes: preparation of diclofenac antibody-doped nanometer-sized silica particles by reverse micelle and sol-gel processing. *Anal Chim Acta*, 2006, 573:

133–137
3 Sato K, Hibara A, Tokeshi M, Hisamoto H, Kitamori T. Microchip-based chemical and biochemical analysis systems. *Adv Drug Delivery Rev*, 2003, 55: 379–391
4 Ibii T, Kaieda M, Hatakeyama S, Shiotsuka H, Watanabe H, Umetsu M, Kumagai I, Imamura T. Direct immobilization of gold-binding antibody fragments for immunosensor applications. *Anal Chem*, 2010, 82: 4229–4235
5 Chai Y, Tian DY, Wang W, Cui H. A novel electrochemiluminescence strategy for ultrasensitive DNA assay using luminol functionalized gold nanoparticles multi-labeling and amplification of gold nanoparticles and biotin-streptavidin system. *Chem Commun*, 2010, 46: 7560–7562
6 Zuo BL, Li SM, Guo Z, Zhang JF, Chen CZ. Piezoelectric immunosensor for sars-associated coronavirus in sputum. *Anal Chem*, 2004, 76: 3536–3540
7 Kurita R, Yokota Y, Sato Y, Mizutani F, Niwa O. On-chip enzyme immunoassay of a cardiac marker using a microfluidic device combined with a portable surface plasmon resonance system. *Anal Chem*, 2006, 78: 5525–5531
8 Kerman K, Nagatani N, Chikae M, Yuhi T, Takamura Y, Tamiya E. Label-free electrochemical immunoassay for the detection of human chorionic gonadotropin hormone. *Anal Chem*, 2006, 78: 5612–5616
9 Fan A, Cao Z, Li H, Kai M, Lu J. Chemiluminescence platforms in immunoassay and DNA analyses. *Anal Sci*, 2009, 25: 587–597
10 Jie GF, Liu B, Pan HC, Zhu JJ, Chen HY. Cds nanocrystal-based electrochemiluminescence biosensor for the detection of low-density lipoprotein by increasing sensitivity with gold nanoparticle amplification. *Anal Chem*, 2007, 79: 5574–5581
11 Li F, Cui H. A label-free electrochemiluminescence aptasensor for thrombin based on novel assembly strategy of oligonucleotide and luminol functionalized gold nanoparticles. *Biosens Bioelectron*, 2013, 39: 261–267
12 Xu S, Liu Y, Wang T, Li J. Positive potential operation of a cathodic electrogenerated chemiluminescence immunosensor based on luminol and graphene for cancer biomarker detection. *Anal Chem*, 2011, 83: 3817–3823
13 Tian CY, Zhao WW, Wang J, Xu JJ, Chen HY. Amplified quenching of electrochemiluminescence from Cds sensitized TiO_2 nanotubes by cdte-carbon nanotube composite for detection of prostate protein antigen in serum. *Analyst*, 2012, 137: 3070–3075
14 Deng SY, Ju HX. Electrogenerated chemiluminescence of nanomaterials for bioanalysis. *Analyst*, 2013, 138: 43–61
15 Richter MM. Electrochemiluminescence (ECL). *Chem Rev*, 2004, 104: 3003–3036
16 Bertoncello P, Forster RJ. Nanostructured materials for electrochemiluminescence (ECL)-based detection methods: recent advances and future perspectives. *Biosens Bioelectron*, 2009, 24: 3191–3200
17 Li F, Yu Y, Cui H, Yang D, Bian Z. Label-free electrochemiluminescence immunosensor for cardiac troponin I using luminol functionalized gold nanoparticles as a sensing platform. *Analyst*, 2013, 138: 1844–1850
18 Shao Y, Wang J, Wu H, Liu J, Aksay IA, Lin Y. Graphene based electrochemical sensors and biosensors: a review. *Electroanalysis*, 2010, 22: 1027–1036
19 Wang Y, Li ZH, Wang J, Li JH, Lin YH. Graphene and graphene oxide: biofunctionalization and applications in biotechnology. *Trends Biotechnol*, 2011, 29: 205–212
20 Kuila T, Bose S, Khanra P, Mishra AK, Kim NH, Lee JH. Recent advances in graphene-based biosensors. *Biosens Bioelectron*, 2011, 26: 4637–4648
21 Zhao C, Feng LY, Xu BL, Ren JS, Qu XG. Synthesis and characterization of red-luminescent graphene oxide functionalized with silica-coated Eu^{3+} complex nanoparticles. *Chem-Eur J*, 2011, 17: 7007–7012
22 Chen GF, Zhai SY, Zhai YL, Zhang K, Yue QL, Wang L, Zhao JS, Wang HS, Liu JF, Jia JB. Preparation of sulfonic-functionalized graphene oxide as ion-exchange material and its application into electrochemiluminescence analysis. *Biosens Bioelectron*, 2011, 26: 3136–3141
23 Shen W, Yu YQ, Shu JN, Cui H. A graphene-based composite material noncovalently functionalized with a chemiluminescence reagent: synthesis and intrinsic chemiluminescence activity. *Chem Commun*, 2012, 48: 2894–2896
24 Cui H, Zou GZ, Lin XQ. Electrochemiluminescence of luminol in alkaline solution at a paraffin-impregnated graphite electrode. *Anal Chem*, 2003, 75: 324–331
25 Frens G. Controlled nucleation for regulation of particle-size in monodisperse gold suspensions. *Nature-Phys Sci*, 1973, 241: 20–22
26 Chu X, Fu X, Chen K, Shen GL, Yu RQ. An electrochemical stripping metalloimmunoassay based on silver-enhanced gold nanoparticle label. *Biosens Bioelectron*, 2005, 20: 1805–1812
27 Lee TMH, Li LL, Hsing IM. Enhanced electrochemical detection of DNA hybridization based on electrode-surface modification. *Langmuir*, 2003, 19: 4338–4343
28 Qiu LP, Wang CC, Hu P, Wu ZS, Shen GL, Yu RQ. A label-free electrochemical immunoassay for igg detection based on the electron transfer. *Talanta*, 2010, 83: 42–47
29 Wang MH, Cao LX, Yan PS, Wu NN. Fabrication and modeling of ultrasensitive label free impedimetric immunosensor for igg based on poly(*o*-phenylenediamine) film modified gold electrode. *Int J Electrochem Sci*, 2012, 7: 7927–7934
30 Qi HL, Wang C, Cheng N. Label-free electrochemical impedance spectroscopy biosensor for the determination of human immunoglobulin g. *Microchim Acta*, 2010, 170: 33–38
31 Dong P, Lin Y, Di J. Fabrication of a label-free plasmon immunosensor based on triangular silver nanoplates. In: *Fourth International Conference on Smart Materials and Nanotechnology in Engineering*. Australia, 2013
32 Peng SS, Zou GZ, Zhang XL. Nanocomposite of electrochemically reduced graphene oxide and gold nanoparticles enhanced electrochemilunescence of peroxydisulfate and its immunosensing abililty towards human igg. *J Electroanal Chem*, 2012, 686: 25–31
33 Li LL, Liu KP, Yang GH, Wang CM, Zhang JR, Zhu JJ. Fabrication of graphene-quantum dots composites for sensitive electrogenerated chemiluminescence immunosensing. *Adv Funct Mater*, 2011, 21: 869–878